Postprint of: Śliwiński P., The basics of design and experimental tests of the commutation unit of a hydraulic satellite motor, Archives of Civil and Mechanical Engineering, Vol. 16, iss. 4 (2016), pp. 634-644, DOI: 10.1016/j.acme.2016.04.003

The basics of design and experimental tests of the commutation unit of a hydraulic satellite motor

Pawel Sliwinski, Ph. D., Eng., e-mail: pawel.sliwinski@pg.gda.pl
Faculty of Mechanical Engineering, Gdansk University of Technology
Narutowicza 11/12 Str., 80-233 Gdansk, Poland

The article presents an analytical method to design the commutation unit in a hydraulic satellite motor. It is shown that the size of the holes feeding the working chambers and their location on the plates closing those chambers depends on the geometrical dimensions of the working mechanism. The overlap in the commutation unit depends on the rotational speed range. It is demonstrated that the geometrical dimensions of the commutation unit clearances change as a function of the angle of machine shaft rotation. The flow in these clearances is described as $Q=f(\Delta p^{\gamma})$. It has been observed that during the transition from the cycle of filling to the cycle of emptying the working chamber, the pressure in the motor's working chamber changes linearly as a function of the shaft rotation angle which has a significant effect on leakage in the commutation unit clearances. The methodology of investigating the commutation unit in a satellite motor and the mathematical model of leakage in the commutation unit clearance described in the article may be successfully adopted to research the commutation unit in positive displacement machines of another type.

Keywords: commutation unit design, commutation unit in a motor, flow in commutation unit clearances, degree of flow laminarity, satellite motor

List of symbols

d_f – root diameter of satellite teeth [mm];
h_s – the clearance height [μm];
k – the coefficient of overlap of inflow/outflow holes in the commutation unit [–];
m – the teeth module [mm];
n – the rotational speed of the motor shaft [rpm];
n_R, n_C – the number of stator, rotor humps;
Δp – the pressure drop in the motor [MPa];
Δp_i – the pressure drop in the working chambers of the motor [MPa];
C, C_1, C_2, C_t – constants;
D_e – the diameter of the inflow and outflow hole in the commutation unit plate [mm];
D_o – the diameter of the inflow and outflow hole in the commutation unit plate for the zero overlap [mm];
J – the geometrical overlap [mm];
L – the clearance length [mm];
Re – the Reynolds number [–];
Q_t – the theoretical displacement of the motor [l/min];
Q_{Cm} – the liquid flow rate in commutation unit clearances [l/min];
Q_C – the volumetric loss caused by the flow of liquid in commutation unit clearances [l/min];
V_g – geometric working volume of the motor [dm^3/rev];
V_t – theoretical working volume of the motor [dm^3/rev];
α – the shaft rotation angle [deg];
α_b – the shaft rotation angle at which the flow Q_{Cm} disappears/is formed in the commutation unit clearance [deg];
γ – the coefficient depending on the flow type;
ν – kinematic viscosity of liquid [mm^2/s];
ρ – liquid density [kg/m^3].

1. Introduction

Each hydraulic positive displacement machine consist of the following units:

a) the working mechanism with working chambers which change their volume when the machine shaft is revolving;
b) a commutation unit, the task of which is to ensure the appropriate process of filling and emptying the chamber of the working mechanism;
c) a unit of internal channels supplying liquid to the commutation unit.

The geometry and kinematics of the working mechanism elements and the process of filling the chambers of this mechanism determines the design solution of the commutation unit node. A hydraulic positive displacement machine of any type should have an original type of the commutation unit node designed specifically this machine. For example:

a) in axial piston displacement machines the commutation unit is composed of a cylinder drum and a directional valve disk [19] or a cylinder sleeve coupled with the cam on the shaft performing a reciprocating motion and cyclically switching the working chamber with the supply or outflow channel [6];
b) in gerotor machines the working mechanism chambers are supplied by: the shaft, a special disk revolving together with the shaft [10,20] or the commutation unit is made of gear wheels and feeding holes in the casing [3,9,9].

Such an original solution of design of the working mechanism and the commutation unit node is also characteristic of the satellite motor [1,12,13,14]. The design and principle of operation of this motor are presented in the next section.

The design solution and the precision of making the commutation unit in each positive displacement machine has a significant impact on:

a) the smoothness of the rotational speed;
b) the smoothness of the torque;
c) the volumetric loss.

Therefore, the design of the commutation unit node for a satellite motor is an important scientific and technical issue. Therefore, four main goals are set for this work:

a) develop a method to design the commutation unit node in a satellite motor;
b) build a motor with a commutation unit made in accordance with the adopted method;
c) perform experimental tests of the motor in order to:
   - verify the commutation unit design methods;
   - confirm the correctness of the flow processes in the commutation unit node;
   - investigate leakage in the commutation unit node;
d) perform a detailed analysis of leakage in the commutation unit and provide a mathematical description of them.

2. Satellite motor

The satellite motor design is presented in Fig. 1. The working mechanism of the satellite motor is a specific gear mechanism in which the rotor is revolving around the shaft axis and the revolving motion is generated by satellites which are coupled with the stator and the rotor (Fig. 2).

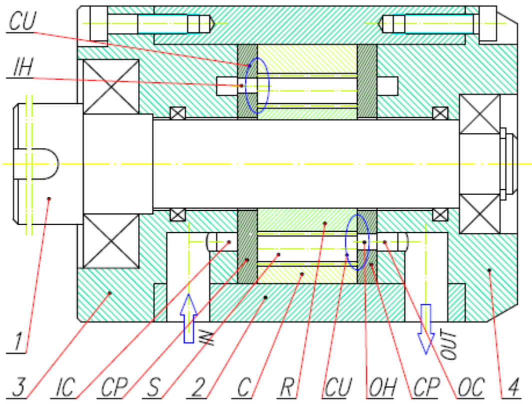

Fig. 1. Satellite motor design: 1 – shaft, 2,3,4 – casing elements, C – stator, R – rotor, S – satellite, CP –commutation plate with holes of liquid inflow IH to and outflow OH from the working chambers,
IC and OC – inlet and outlet manifold, CU – commutation unit.

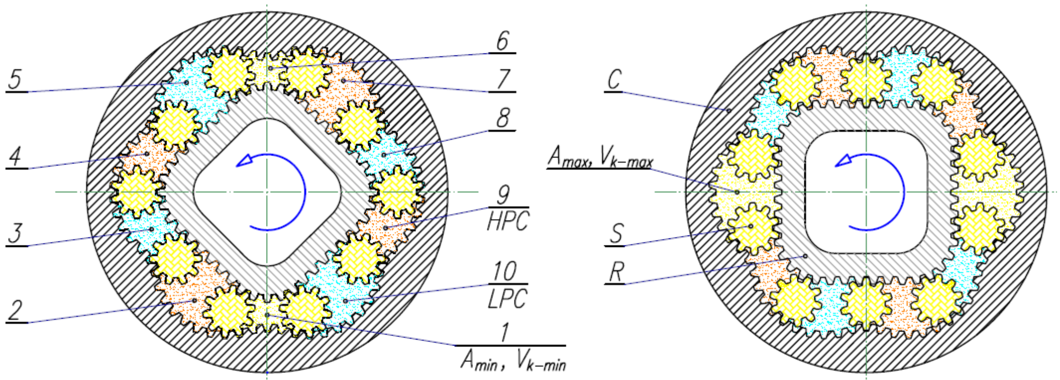

Fig. 2. The working mechanism of a satellite motor: C – stator, R – rotor, S – satellite, 1÷10 – working chambers; other symbols – a description in the text.

The stator teeth are inside and it has six humps (n_C=6). The rotor teeth are outside and it has four humps (n_R=4). The gear wheels called satellites work with the stator and the rotor. Spaces called working chambers are formed between the satellites, the stator and the rotor. The number of the working chambers is equal to the number of the satellites.

During the rotor rotation the working chambers:

a) change their volume from minimum $V_{k\text{-}min}$ to maximum $V_{k\text{-}max}$ forming a high pressure chamber HPC;
b) change their volume from maximum $V_{k\text{-}max}$ to minimum $V_{k\text{-}min}$ forming a low pressure chamber LPC.

The number of filling and emptying cycles of the working chambers per one rotation of the shaft, z_c, is:

$$z_c = n_C \cdot n_R \tag{1}$$

The shaft rotation angle α_{DC} in respect of which the change from $V_{k\text{-}min}$ do $V_{k\text{-}max}$ takes place, is:

$$\alpha_{DC} = \pi \cdot \frac{z_k}{z_c} \text{ [rad]} \tag{2}$$

Hence, 24 cycles of filling and emptying of chambers correspond to one shaft rotation, for the mechanism as in Fig. 2, α_{DC}=75°.

The total displacement Q of the motor engine is the sum of:

$$Q = \underbrace{V_t \cdot n}_{Q_t} + \underbrace{Q_{Lfg} + Q_C}_{Q_L} \tag{3}$$

where:
- V_t – the theoretical working volume (usually V_t~V_g);
- Q_t – the theoretical displacement of the motor;
- Q_{Lfg} – the component of volumetric losses – the liquid flow rate in flat clearances of the working mechanism of the motor;
- Q_C – the component of volumetric losses - the liquid flow rate in flat clearances of the commutation unit of the motor;
- Q_L – the volumetric losses.

In a hydraulic motor, for Q=const, an increase in the motor load will result in an increase in leakage Q_c and Q_{Lfg}, and as a result, in lowering the rotational speed of the motor.

3. The commutation unit in a satellite motor and a method to design it

A correct process of filling the working chambers of the satellite mechanism is ensured by the commutation unit. The commutation unit comprises satellites S and inflow IH and outflow OH holes in commutation plates CP (Fig. 3). During the motor shaft rotation the satellites are moving and properly cover the inflow holes IH or open the outflow holes OH in the commutation plates CP.

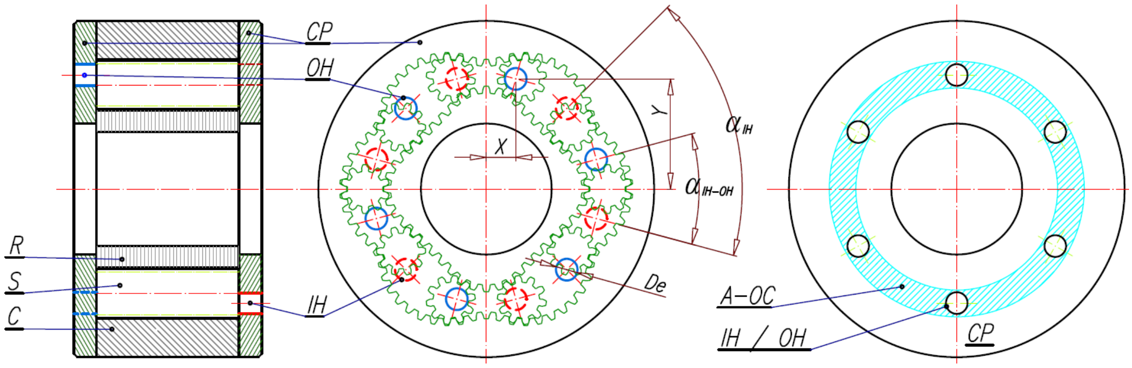

Fig. 3. Location of inflow IH and outflow OH holes in commutation plates. A–OC – the contact area of liquid and the supplying manifold or the outflow manifold.

The position of inflow and outflow holes (X,Y) on the commutation plates relative to the centre of rotor rotation and the hole diameter D_e (Fig. 3) depend on the position of the satellites in the mechanism corresponding to field A_{min} and field A_{max} (Fig. 4).

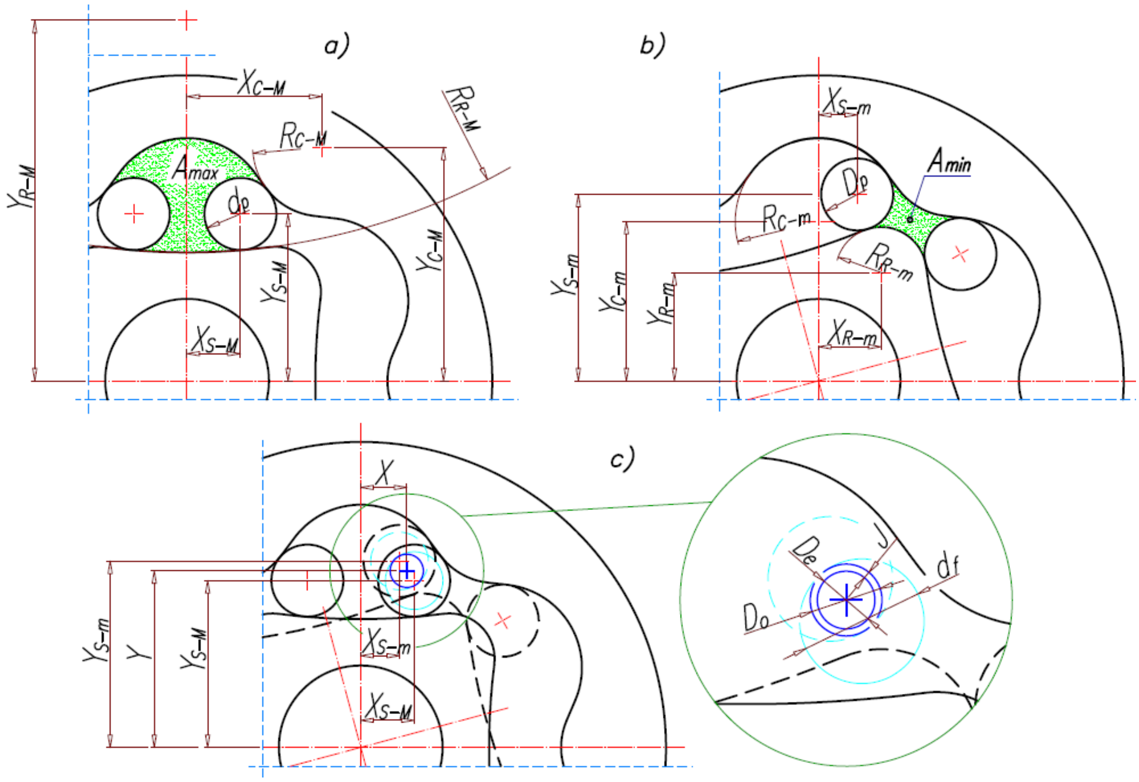

Fig. 4. Characteristic dimensions of the satellite mechanism to determine the satellite position for: a) A_{max}, b) A_{min} and c) the inflow/outflow hole position on the commutation plate and its diameter.

The characteristic dimensions required to:

a) calculate the position of the satellite ($X_{S\text{-}m}$ and $Y_{S\text{-}m}$) relative to the centre of rotor rotation for A_{min} are the following (Fig. 4):
   - $R_{C\text{-}m}$ and $R_{R\text{-}m}$ – the radius of the reference circle of the stator and rotor teeth within A_{min} [mm];
   - $X_{R\text{-}m}$, $Y_{R\text{-}m}$ – the coordinates of the reference circle of the rotor teeth within A_{min} [mm];
   - $X_{C\text{-}m}$, $Y_{C\text{-}m}$ – the coordinates of the reference circle of the stator teeth within A_{min} [mm];

b) calculate the position of the satellite ($X_{S\text{-}M}$ and $Y_{S\text{-}M}$) relative to the centre of rotor rotation for A_{max} are the following (Fig. 4):
   - $R_{C\text{-}M}$ and $R_{R\text{-}M}$ – the radius of the reference circle of the stator and rotor teeth within A_{max} [mm];
   - $X_{R\text{-}M}$, $Y_{R\text{-}M}$ – the coordinates of the reference circle of the rotor teeth within A_{max} [mm];
   - $X_{C\text{-}M}$, $Y_{C\text{-}M}$ – the coordinates of the reference circle of the stator teeth within A_{max} [mm].

The position of the satellite relative to the centre of rotor rotation can be calculated from the relation:

a) for the minimum chamber (A_{min}) (Fig. 4):

$$X_{S-m} = \left(R_{C-m} - 0.5 \cdot d_p\right) \cdot \left(\sin(\arccos A_1) \cdot A_2 + A_1 \cdot A_3\right) \tag{4}$$

$$Y_{S-m} = Y_{C-m} - \left(R_{C-m} - 0.5 \cdot d_p\right) \cdot \left(A \cdot B - \sin(\arccos A) \cdot C\right) \tag{5}$$

where:

$$A_1 = \frac{R_{C-m}^2 - R_{R-m}^2 - d_p \cdot (R_{C-m} + R_{R-m}) + (Y_{C-m} - Y_{R-m})^2 + X_{R-m}^2}{(2 \cdot R_{C-m} - d_p) \cdot \sqrt{(Y_{C-m} - Y_{R-m})^2 + X_{R-m}^2}} \tag{6}$$

$$A_2 = \frac{Y_{C-m} - Y_{R-m}}{\sqrt{(Y_{C-m} - Y_{R-m})^2 + X_{R-m}^2}} \tag{7}$$

$$A_3 = \frac{X_{R-m}}{\sqrt{(Y_{C-m} - Y_{R-m})^2 + X_{R-m}^2}} \tag{8}$$

b) for the maximum chamber (A_{max}) (Fig. 4):

$$X_{S-M} = \left(R_{R-M} - 0.5 \cdot d_p\right) \cdot (A_4 \cdot A_5 - \sin(\arccos A_4) \cdot A_6) \tag{9}$$

$$Y_{S-M} = Y_{R-M} - \left(R_{R-M} - 0.5 \cdot d_p\right) \cdot (A_4 \cdot A_5 + \sin(\arccos A_4) \cdot A_6) \tag{10}$$

where:

$$A_4 = \frac{R_{R-M}^2 - R_{C-M}^2 - d_p \cdot (R_{C-M} + R_{R-M}) + (Y_{R-M} - Y_{C-M})^2 + X_{C-M}^2}{(2 \cdot R_{C-M} + d_p) \cdot \sqrt{(Y_{R-M} - Y_{C-M})^2 + X_{C-M}^2}} \tag{11}$$

$$A_5 = \frac{Y_{R-M} - Y_{C-M}}{\sqrt{(Y_{R-M} - Y_{C-M})^2 + X_{C-M}^2}} \tag{12}$$

$$A_6 = \frac{X_{C-M}}{\sqrt{(Y_{R-M} - Y_{C-M})^2 + X_{C-M}^2}} \tag{13}$$

The position of the centre of the inflow (or outflow) hole in the commutation plate relative to the rotor rotation axis (Fig. 4) is calculated from the relation:

$$X = \frac{X_{S-m} + X_{S-M}}{2} \tag{14}$$

$$Y = \frac{Y_{S-m} + Y_{S-M}}{2} \tag{15}$$

As it follows from Fig. 4 the position of the inflow/outflow hole in the commutation plate does not depend on the angular position of the rotor and has a definite position only relative to the stator hump. Hence, the conclusion that:

– the number of IH or OH holes in the commutation plate is equal to the number n_C of the stator humps;
– the angle α_{IH} (Fig. 3) between inflow holes IH in the commutation plate measured relative to the centre of the stator (or the rotor) is identical. Likewise, angle α_{OH} (Fig. 3) between outflow holes OH is also identical. Namely:

$$\alpha_{IH} = \alpha_{OH} = 2 \cdot \frac{\pi}{n_o} \quad \text{[rad]} \tag{16}$$

– angle α_{IH-OH} between IH and OH is:

$$\alpha_{IH-OH} = \frac{\pi}{n_o} \quad \text{[rad]} \tag{17}$$

The diameter of IH (or OH) is:

$$D_e = \underbrace{d_f - 2 \cdot \sqrt{(X_{S-m} - X_{S-M})^2 + (Y_{S-m} - Y_{S-M})^2}}_{D_o} - 2 \cdot J \tag{18}$$

where J is the IH (or OH) overlap by the satellite defined as:

$$J = k \cdot m \tag{19}$$

k is the overlap coefficient of:

a) k=0 – the hole overlap by the satellite is zero, and then $D_e=D_o$ (Fig. 5a));
b) k<0 – the hole overlap by the satellite is negative (Fig. 5b)) and then $D_e>D_o$;

c) $k>0$ – the hole overlap by the satellite is positive (Fig. 5c)) and then $D_e<D_o$.

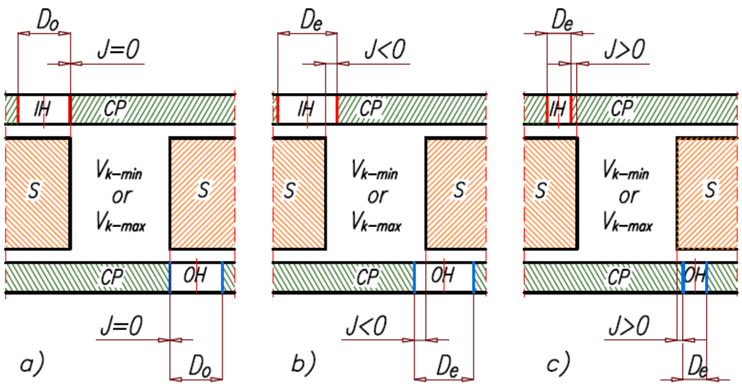

Fig. 5. Overlaps in the satellite mechanism commutation unit: a) zero ($k=0$), b) negative ($k<0$), c) positive ($k>0$).

4. Commutation unit clearances

Fig. 6 presents the process of passage of the low-pressure working chamber LPC through the minimum chamber $V_{k\text{-min}}$ into the high-pressure working chamber HPC. Two commutation unit clearances are formed during this process. There is leakage in these clearances:

a) Q_{Cm1} – from channel IH to chamber $V_{k\text{-min}}$, caused by the pressure difference Δp_1;

b) Q_{Cm2} – from chamber $V_{k\text{-min}}$ to channel OH, caused by the pressure difference Δp_2.

The leakage occurs in the range of a very small shaft rotation angle $\alpha=(-\alpha_b;+\alpha_b)$. For further considerations, it is assumed that:

a) the angular shaft position $\alpha=0^o$ corresponds to chamber $V_{k\text{-min}}$ or chamber $V_{k\text{-max}}$;

b) angle α_b is the critical value of angle α, for which $Q_{Cm1}= Q_{Cm2}=0$.

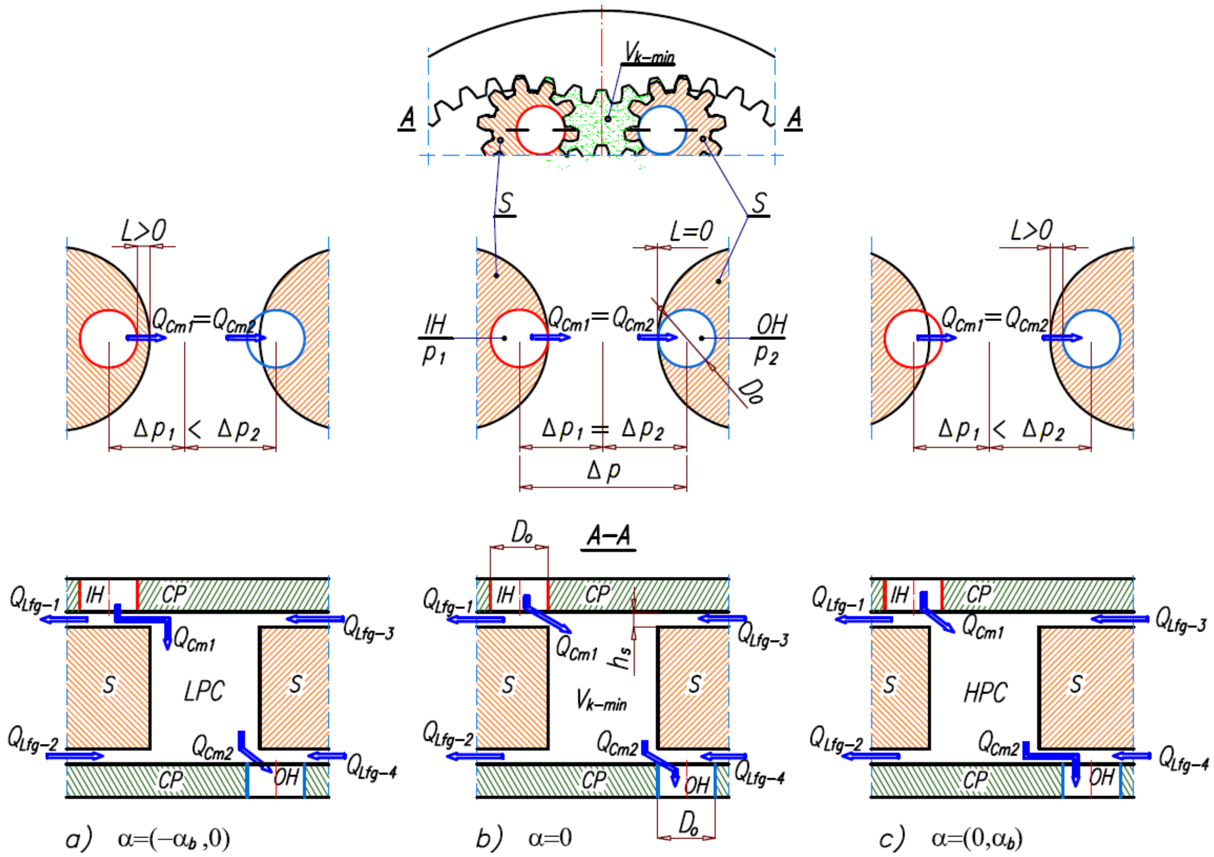

Fig. 6. Process of LPC transition to HPC via $V_{k\text{-min}}$. a) final phase of reducing the LPC volume ($\alpha=(-\alpha_b,0)$); b) chamber $V_{k\text{-min}}$ ($\alpha=0$); c) initial phase of increasing the HPC volume ($\alpha=(0,\alpha_b)$). Description in the text.

The clearance length L in the satellite mechanism (Fig. 6) is a function of module m and angle α [1]:

$$L = 0.213 \cdot m \cdot \alpha \tag{20}$$

If $\alpha = \alpha_b$, then:

$$L = L_{max} = 0.213 \cdot m \cdot \alpha_b \tag{21}$$

Therefore, it is possible to choose such a positive overlap value k, for which $Q_{Cm}=0$ at $\alpha=0$. Hence:

$$J = 2 \cdot L \tag{22}$$

that is:

$$k = 0.213 \cdot \alpha \tag{23}$$

If $\alpha > \alpha_b$, then the commutation unit clearance passes through a flat clearance created by the satellite head and the commutation plate. In such a clearance there is leakage Q_{Lfg}, shown in Fig. 6. A detailed description of leakage Q_{Lfg} is presented in [11].
Commutation unit clearances are arranged serially. For such a case:

$$Q_{Cm1} = Q_{Cm2} = Q_{Cm} \tag{24}$$

$$\Delta p_1 + \Delta p_2 = \Delta p \tag{25}$$

5. Known methods of description of flow in commutation unit clearances in positive displacement machines

Commutation unit clearances are clearances small in length or with length equal to zero (Fig. 6). The geometry of these clearances changes during the shaft rotation. Hence, it is assumed that a not-fully developed turbulent flow occurs in these clearances.
So far, the analysis of flows in commutation unit clearances has been disregarded by researchers of hydraulic positive displacement machines. A mathematical description of flows in commutation unit clearances in such machines is not to be found in the literature. In the literature, volumetric losses are described globally, without specifying the type of clearances [2,7,15].
Liquid flows in clearances of the commutation unit of a hydraulic motor are a typical case of flow in:
– the sharp-edged clearance (orifice type – Fig. 7);
– the flat clearance which is very small in length.
In the literature, the flow in the orifice is described in the general form as:

$$Q = C_t \cdot A_S \cdot \sqrt{\frac{2}{\rho} \cdot \Delta p} \tag{26}$$

where it is assumed that C_t=f(Re) [4,5,16,17,18]. For example, in accordance with [17,18] the flow rate in the clearances of valves (Fig. 7 and Fig. 8) is described by the following formula, in which:

$$C_t = C_{d\infty} \cdot \left(1 + a \cdot e^{\frac{-\delta_1}{C_{d\infty}} \cdot \sqrt{Re}} + b \cdot e^{\frac{-\delta_2}{C_{d\infty}} \cdot \sqrt{Re}}\right) \tag{27}$$

where:
– a, b, δ_1, δ_2 – coefficients depending on the flow type;
– $C_{d\infty}$ – the turbulent flow coefficient.

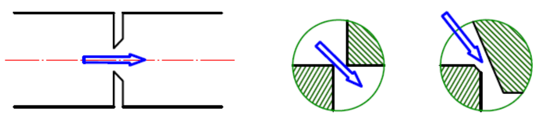

Fig. 7. Different types of holes: orifice, sharp-edged clearance and valve clearance [18].

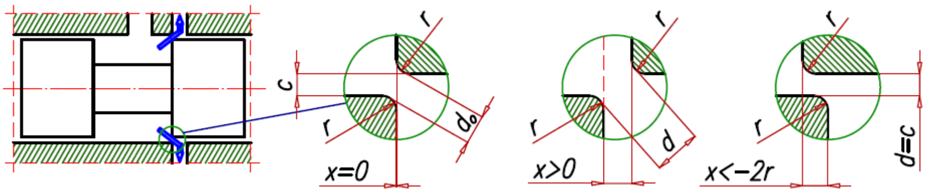

Fig. 8. Annular gaps of the directional valve spool and the effect of the spool position on the clearance size and geometry [17].

In the literature concerning hydraulic positive displacement machines the flow in the commutation unit is described depending on the machine type. Thus:
a) in hydraulic motors the flow in the commutation unit is described as [2,15]:
   – a mean value independent of the angle of the shaft rotation;
   – turbulent flow and it is referred to the theoretical working volume V_t:

$$Q = C_t \cdot \sqrt{\frac{2}{\rho} \cdot \Delta p} \cdot \sqrt[3]{\left(\frac{V_t}{2 \cdot \pi}\right)^2} \tag{28}$$

b) in axial piston pumps the flow in the commutation unit is described as [19]:
   – a mean value independent of the angle of the shaft rotation;

– a laminar flow independent of the geometrical dimensions of the clearance.

The above described methods cannot be used to describe the flow in the motor commutation unit clearances as:

– it is an implicit equation (C_t=f(Re)=f(Q_c));
– there is a laminar component at low liquid flow rates in the clearance. Consequently, it is not appropriate to describe a partially turbulent flow as function $\Delta p^{0.5}$;
– the dimensions of clearances in the commutation unit change as a function of the shaft rotation angle α.

6. A mathematical model of liquid flow in commutation unit clearances

When developing a new mathematical model of the liquid flow rate Q_{cm} in commutation unit clearances, the following assumptions were adopted:

a) the flow in motor commutation unit clearances within the range $\alpha=(0,+\alpha_b)$ (Fig. 6) may be written using the generally known formula:

$$Q_{Cm} = C_2 \cdot \Delta {p_2}^{\gamma} \tag{29}$$

in which γ is the coefficient taking the value from the range (0.5;1) [11], and C is a constant dependent on the geometric dimensions of the clearance and the parameters of the liquid. For $\alpha=(-\alpha_b;0)$:

$$Q_{Cm} = C_1 \cdot \Delta {p_1}^{\gamma} \tag{30}$$

b) at the moment of a change of the commutation unit phase there is a linear change in pressure in the chambers which was confirmed by the results of experimental tests (Fig. 13). Then Δp_1 and Δp_2 (Fig. 13) may be described by the formulas:

$$\Delta p_1 = \frac{\Delta p}{2} \cdot \left(1 - \frac{\alpha}{\alpha_b}\right) \tag{31}$$

$$\Delta p_2 = \frac{\Delta p}{2} \cdot \left(1 + \frac{\alpha}{\alpha_b}\right) \tag{32}$$

where α_b is the shaft rotation critical angle for which there is a linear change of pressure in the working chamber.

In [11] it has been demonstrated that:

$$C_1 = C_2 = b \cdot \left(\frac{1}{\nu}\right)^{\left(2-\frac{1}{\gamma}\right)} \cdot \left(\frac{1}{K \cdot \rho}\right)^{\gamma} \cdot \left(\frac{2 \cdot {h_s}^3}{L_r}\right)^{\gamma} \tag{33}$$

where L_r is the replacement length of the clearance (Fig. 6) expressed by the formula:

$$L_r = \frac{D_e}{2} + 0.213 \cdot m \cdot \alpha \tag{34}$$

Assuming that b=D_e and considering the relation (32), (33) and (34) in the formula (29) we obtain:

$$Q_{Cm} = \underbrace{D_e \cdot \left(\frac{1}{\nu}\right)^{\left(2-\frac{1}{\gamma}\right)} \cdot \left(\frac{2 \cdot {h_s}^3 \cdot (\alpha_b + \alpha)}{K \cdot \alpha_b \cdot \rho \cdot (D_e + 0.426 \cdot m \cdot \alpha)}\right)^{\gamma}}_{C} \cdot \Delta p^{\gamma} \tag{35}$$

The above formula contains coefficient K the value of which cannot be defined by way of theoretical analysis [11]. The value of this coefficient is calculated on the basis of the experimentally obtained value of constant C.

Coefficient γ characterizes the flow type and depends on the geometric dimensions of the clearance and is a function of angle α of the shaft rotation. Furthermore, this coefficient depends on the liquid viscosity μ. Hence, γ=f(μ,L). Theoretically, the function describing the relationship between γ and μ and L should take the asymptotic values of 0.5 and 1. The arctan function, modified appropriately, has such features [8]. Therefore, it is proposed to describe coefficient γ by the formula, empirically determined in the form:

$$\gamma = 0.5 \cdot \left(2.5 \cdot \frac{\mu}{\mu_R}\right)^{\frac{\alpha}{4}} \cdot arctg\left(\left(0.1 + \frac{\alpha}{\alpha_R}\right)^{\left(\frac{\mu_R}{5\cdot\mu}\right)^2} - 0.5\right) + 0.75 \tag{36}$$

in which μ_R is the reference dynamic viscosity. It has been assumed that μ_R = 100mPas.
During one complete rotation of the shaft the number of flow peaks Q_{Cm} is equal to the number z_c of working chamber filling and emptying. Thus, for a mechanism with n_C=6 and n_R=4 the number of peaks of leakage Q_{Cm} is equal to 24.
As Q_{cm} depends on α the mean value Q_{cm-av} of this flow in the range $\alpha=(-\alpha_b;+\alpha_b)$ is:

$$Q_{Cm-av} = \frac{1}{2\cdot\alpha_b} \cdot \int_{-\alpha_b}^{+\alpha_b} Q_{Cm}\, d\alpha \approx \frac{1}{2} \cdot D_e^{(1-\gamma)} \cdot \left(\frac{1}{\nu}\right)^{\left(2-\frac{1}{\gamma}\right)} \cdot \left(\frac{2}{K} \cdot \frac{h_s^{\,3}}{\rho}\right)^{\gamma} \cdot \Delta p^{\gamma} \tag{37}$$

The mean value of flow in the clearances of the commutation unit during one rotation of the shaft is:

$$Q_C = n_C \cdot n_R \cdot \frac{\alpha_b}{\pi} \cdot Q_{Cm-av} \tag{38}$$

7. The investigated motor and the measuring system

A satellite motor prototype with the parameters shown in Tab. 1 was designed (Fig. 1) and built for experimental tests.

Tab. 1. Satellite motor parameters and inflow/outflow hole position (acc. to Fig. 2)

V_t	m	z	h_s	D_e	X	Y
[cm^3/rev]	[mm]	[-]	[um]	[mm]	[mm]	[mm]
32.94	0.75	10	5.35	3.93	5.16	18.88

In order to experimentally determine the flow rate Q_{Cm} in commutation unit clearances it was necessary to measure the motor instantaneous displacement Q with the small constant rotational speed n and with the constant pressure drop Δp in the motor. For that purpose the motor shaft was coupled the with worm gear WG (Fig. 9). This gear is driven by the electric motor E. The motor tests were conducted with the constant rotational speed of n = 1 rpm.

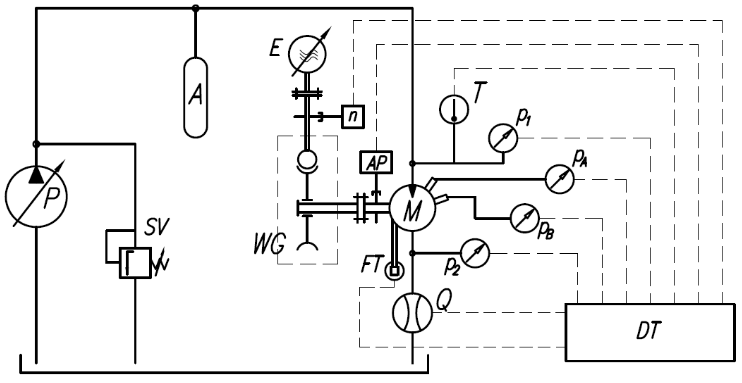

Fig. 9. Measuring system diagram: M – investigated motor, P – pump, A – accumulator, E – electrical motor, SV – safety valve, WG – worm gear, DT – measurement data recorder, Q – flow meter, FT – force sensor (for moment measurement), p_1, p_2, p_A and p_B – pressure sensors, T – temperature sensor, n_1 – rotational speed sensor, AP – angular shaft position sensor.

In order to measure the pressure in the working chambers at the moment of opening and closing the OH and IH holes by the satellites, pressure sensors p_A and p_B were located in the working mechanism as in Fig. 10.

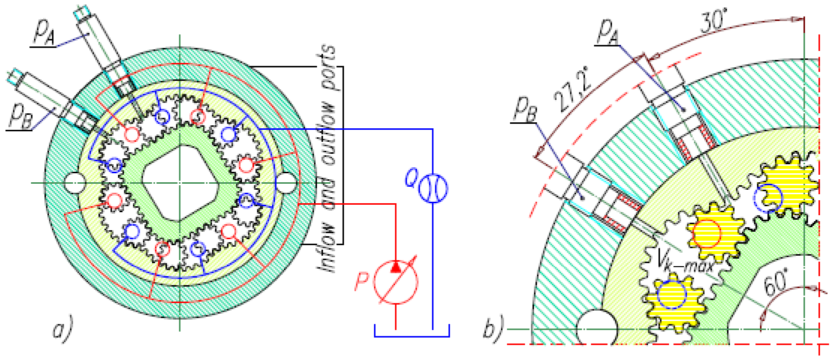

Fig. 10. Method of measuring motor displacement Q and pressure in working chambers.

The motor was tested using the Total Azolla 46 oil (ν=40cSt, ρ=873kg/m^3).

8. Results of experimental research

It was observed that during one full rotation of the shaft, there were 12 peaks of flow rate Q_{Cm} with large values and 12 peaks of flow rate Q_{Cm} with small values. 24 peaks in total (Fig. 11). That is, as many as there are filling and emptying cycles of working chambers per one rotation of the shaft. In Fig. 11 flow rate peaks with large values have been marked as Q_{Cm-H} and flow peaks with small values as Q_{Cm-L}. The relation of the values of these peaks is:

$$\frac{Q_{Cm-H}}{Q_{Cm-L}} \approx 2.5 \tag{39}$$

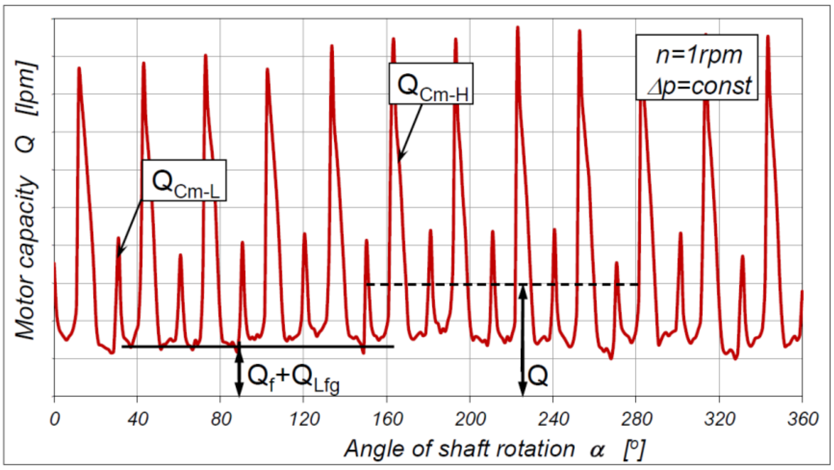

Fig. 11. Characteristics Q=f(α) of loaded motor at n=1 rpm.

In [14] it is shown that Q_{Cm-L} and Q_{Cm-H} result from:

– the movement of satellites within the backlash;

– errors in the manufacture of toothed curves of the rotor, stator and satellites.

Due to the fact that the rotational speed of the motor is very small, the pressure drop in the internal channels of the motor can be omitted and then the pressure drop in the working chambers Δp_i is equal to:

$$\Delta p_i = \Delta p = p_1 - p_2 \tag{40}$$

The results show, that (according to the assumptions made in Chapter 5 (designs (40) and (41)) there is a linear change in pressure in the working chambers at the moment of changing the commutation unit phase (Fig. 12 and Fig. 13).

In Fig. 13 it is assumed that $\alpha=0^o$ corresponds to such a position of the operating mechanism, for which there is a $V_{k\text{-}max}$ chamber, or possibly a $V_{k\text{-}min}$ chamber. Then, the overlap in tested motor is.

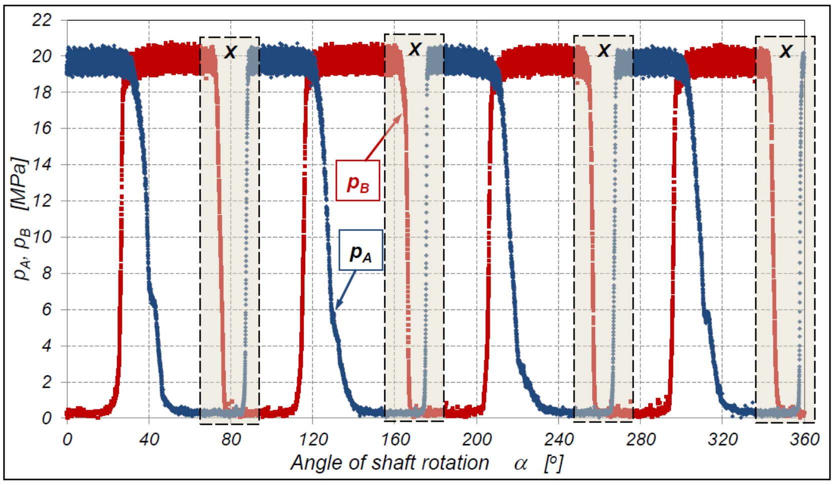

Fig. 12. Characteristics of $p_A=f(\alpha)$ and $p_B=f(\alpha)$. Supply pressure 20 MPa.

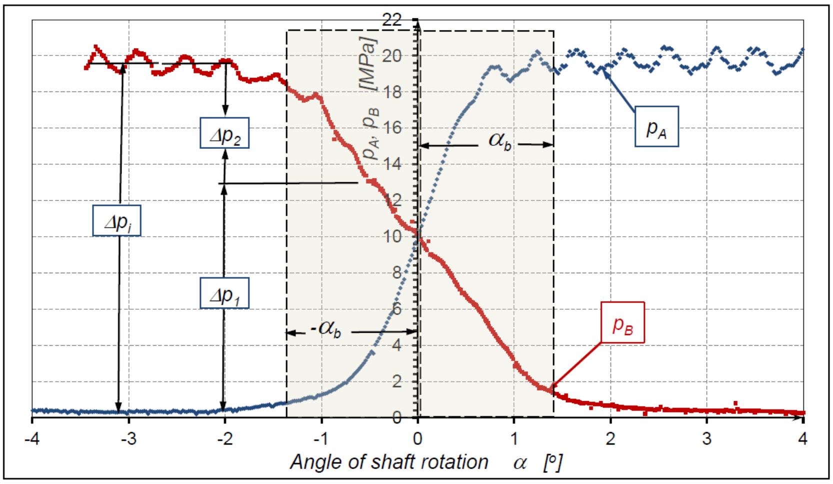

Fig. 13. Area X from Fig. 12. The course of pressure in the working chamber during passage through $V_{k\text{-}min}$ (characteristics $p_A = f(\alpha)$) and through $V_{k\text{-}max}$ (characteristics $p_B = f(\alpha)$).

As it follows from Fig. 13 that the angle within the range of which the peak increases or decreases is small being $\alpha=\alpha_b=1.3^o$. Hence, for $\alpha_b=1.3^o$ $Q_{cm\text{-}H} \sim 0$ and $Q_{cm\text{-}L} \sim 0$.

Further analyses were carried out for peaks of flow $Q_{Cm\text{-}H}$ with higher values. For the case of peaks of flow $Q_{Cm\text{-}L}$ with lower values the analysis is the same.

The experimental characteristics of $Q_{Cm\text{-}H}=f(\alpha>0)$ are shown in Fig. 14. For $\alpha<0$ the shape of characteristics $Q_{Cm\text{-}H}=f(\alpha<0)$ is a mirror reflection of the characteristics $Q_{Cm\text{-}H}=f(\alpha>0)$. While

Fig. 15 shows the characteristics $Q_{Cm-H}=f(\Delta p)$. The values of constant C and coefficient γ appearing in formula (35), determined on the basis of experimental data. are shown in Fig. 16. It was also observed that the flow disturbance in clearances of the commutation unit was becoming smaller with the increasing angle of rotation.

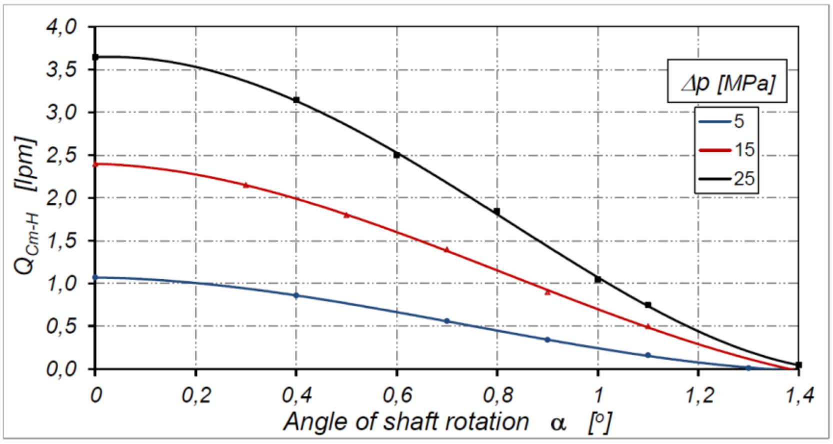

Fig. 14. Characteristics $Q_{Cm-H}=f(\alpha)$ at Δp=const.

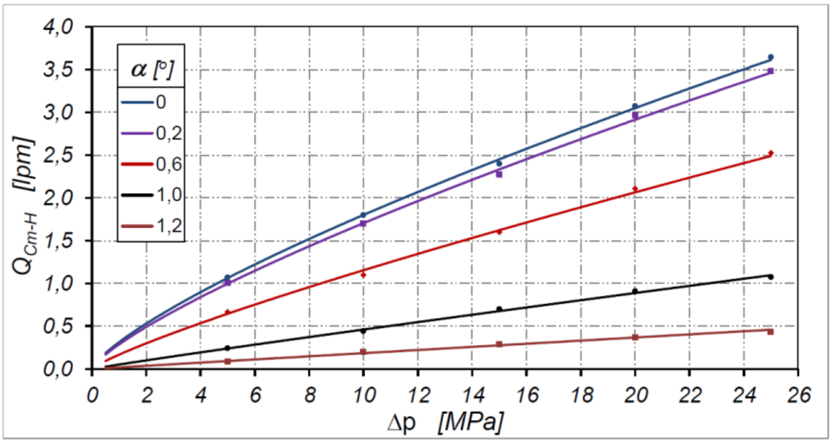

Fig. 15. Characteristics $Q_{Cm-H}=f(\Delta p)$ at α=const.

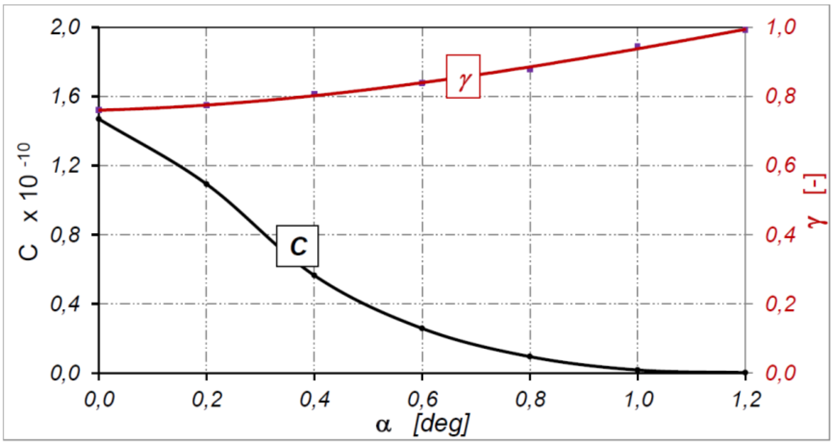

Fig. 16. Characteristics of $C=f(\alpha)$ and $\gamma=f(\alpha)$.

The difference in the values of coefficient γ calculated according to (36) and obtained experimentally (Fig. 16) is approx. 8.5%. As a result, the flow rate Q_{Cm}, calculated according to (46) will be also imprecise (Fig. 17). In the range up to α=0.2 the difference reaches 38%.

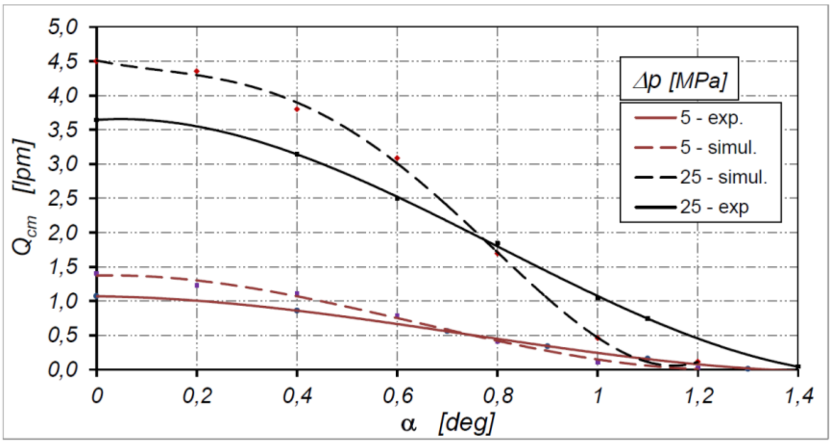

Fig. 17. Comparison of Q_{Cm} calculated in accordance with (35) with the value obtained experimentally.

Bearing in mind the results of experimental tests (Fig. 11), the mean value of the flow rate in commutation unit clearances during one shaft rotation should be expressed by the formula:

$$Q_C = n_C \cdot n_R \cdot \frac{\alpha_b}{2 \cdot \pi} \cdot (Q_{Cm-\mathrm{H}-av} + Q_{Cm-\mathrm{L}-av}) \tag{41}$$

The values $Q_{Cm\text{-}H\text{-}av}$ and $Q_{Cm\text{-}L\text{-}av}$ are calculated according to formula (37).
Assuming similarly to (39):

$$\frac{Q_{Cm-H-av}}{Q_{Cm-L-av}} \approx 2.5 \tag{42}$$

and considering equations (37), the formula (41) takes the form:

$$Q_C = \frac{3.5}{10 \cdot \pi} \cdot n_C \cdot n_R \cdot \alpha_b \cdot {D_e}^{(1-\gamma)} \cdot \left(\frac{1}{\nu}\right)^{\left(2-\frac{1}{\gamma}\right)} \cdot \left(\frac{2}{K} \cdot \frac{{h_s}^3}{\rho}\right)^{\gamma} \cdot \Delta p^{\gamma} \tag{43}$$

For the analysed satellite motor commutation unit, according to the experimental data, for α=0 is: γ=0.76, K=10.25·10^4. Then:

$$Q_C = 15.98 \cdot 10^{-6} \cdot {D_e}^{0.24} \cdot {h_s}^{2.28} \cdot \left(\frac{1}{\nu}\right)^{0.68} \left(\frac{1}{\rho}\right)^{0.76} \cdot \Delta p^{0.76} \tag{44}$$

Characteristics Q_c obtained based on experimental data and calculated from the above relationships are shown in Fig. 18. It can be seen that the values of the mean oil flow rate Q_c in the clearances of the commutation unit, calculated from the relation (44) are slightly higher than those determined experimentally. With Δp=25MPa the difference is only 3%. This proves that the adopted assumptions and simplifications were correct.

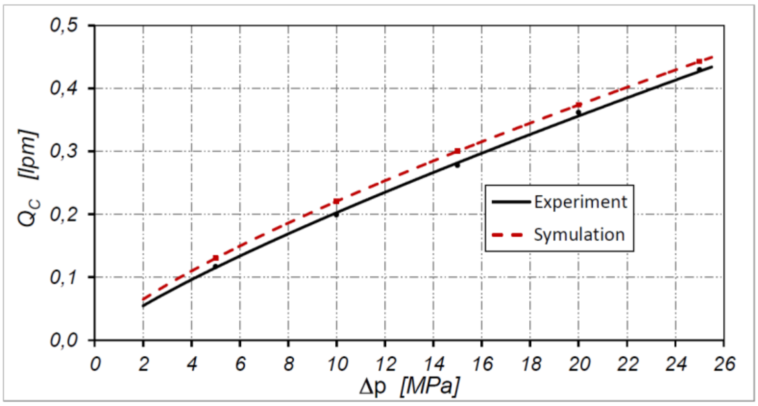

Fig. 18. Comparison of components of volumetric losses Q_C determined experimentally and calculated according to the formula (44).

The effect of the hole diameter D_e on the flow rate $Q_{cm\text{-}H}$, at α=0, is presented in Fig. 19.

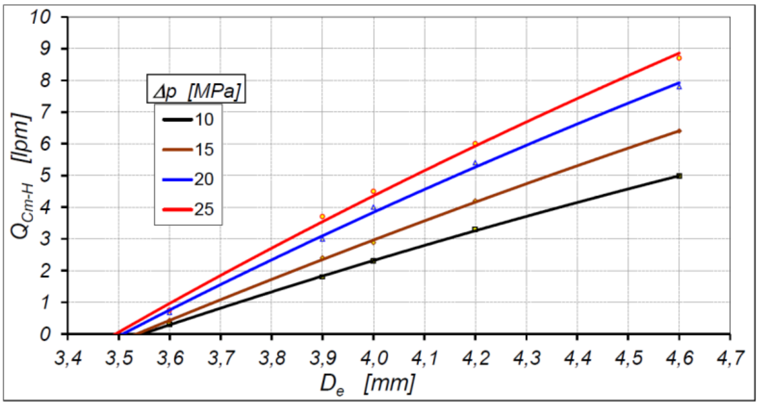

Fig. 19. Flow rate $Q_{Cm\text{-}H}=f(D_e)$, at α=0 and Δp=const.

Hence, it is possible to choose diameter D_e of holes in the commutation plate CP for which $Q_{cm\text{-}H}=0$ at $\alpha=0$. Hence, for $Q_{Cm\text{-}H}=0$ inflow and outflow holes, D_e=3.5mm in diameter, should be made in the compensation plates. Therefore, a positive overlap of the hole by the satellite, J=0.2mm in size, is achieved (k=0,278). Such value is desirable in a low speed motor. In motors operating at higher speeds, the zero overlap should be used [1], possibly a small negative overlap (k=0.05). In this way it will be possible to avoid an unfavourable pressure increase in the minimum chamber $V_{k\text{-}min}$. Moreover, the flow rate Q_c will have a very small share in the actual displacement Q of the motor (formula (3)) whereby the increase in the volumetric efficiency will be insignificant.

9. Summary

The objective of the article was to describe an analytical method for designing the commutation unit in a satellite motor, describe the results of commutation unit tests and develop new mathematical formulas describing the flow in commutation unit clearances. This objective has been was fully accomplished.

The results of experimental tests of the SM satellite motor prototypes have confirmed that:

– the theoretical relations for designing the motor commutation unit are correct;
– the design solution of the commutation unit is correct and the operation of the commutation unit in the motor is correct;

– the flow rate Q_{cm} in commutation unit clearances is variable as a function of the shaft rotation function and for $\alpha=\alpha_b=1.3^o$ Q_{Cm} is close to zero (Fig. 11 and Fig. 14);
– the flow in the commutation unit clearance is not fully developed and turbulent in nature (γ=0.76) and depends on the working liquid parameters, axial clearances of satellites in the working mechanism and the diameter of the inflow (or outflow) hole in the commutation unit plate.

The mathematical formulas presented in the article can be adopted to describe leakages in the commutation unit of hydraulic machines of a different type, for example, in gerotor motors or piston motors.

10. References

1. A. Balawender, P. Sliwinski and others: Developmental research of hydraulic satellite motors and satellite pump with small geometrical displacement supplied with water, emulsion and oil (in Polish). Report of research project No. R0300103. Gdansk University of Technology, 2010.
2. A. Balawender: Physical and mathematical model of losses in hydraulic motors. Developments in mechanical engineering, Gdansk University of Technology Publishers. Gdansk 2005.
3. S. Bednarczyk, J. Stryczek: Development of gerotor pumps (in Polish). Hydraulika i Pneumatyka, No. 1/2000.
4. A. Ellman, R. Piche: A two regime orifice flow formula for numerical simulation. Journal of Dynamic Systems, Measurement and Control. Vol. 121/721, 12/1999.
5. M. Jelali, A. Kroll: Hydraulic Servo-systems: Modelling, Identification and Control. Springer-Verlag London Berlin Heidelberg, 2004.
6. L. Osiecki: Commutation units of hydraulic axial piston machines. Gdansk University of Technology Publishers, Gdansk 2006.
7. P. Osinski, A. Deptuła, M. A. Partyka: Discrete optimization of a gear pump after tooth root undercutting by means of multi-valued logic trees. Archives of Civil and Mechanical Engineering, No. 13/2013.
8. P. Patrosz P: PhD thesis (in progress): Compensation of pressure peaks in piston pump with cam driven commutation unit. Gdansk University of Technology.
9. J. Stryczek, S. Bednarczyk, K. Biernacki: Gerotor pump with POM gears: Design, production technology, research. Archives of Civil and Mechanical Engineering, No. 14/2014.
10. J. Stryczek: Gears of the Hydraulic Machines (in Polish), Publishing House of Wroclaw University of Technology, Wroclaw, 2007.
11. P. Sliwinski: The flow of liquid in flat gaps of satellite motors working mechanism. Polish Maritime Research, No. 2/2014.
12. P. Sliwinski, P. Patrosz: Diagnostics of commutation unit in satellite pumps and motors. Hydraulika a Pneumatika, No. 1-2/2013.
13. P. Sliwinski: R&D of satellite pumps and motors with small geometrical displacement supplied with oil and non-flammable liquids. Developments in mechanical engineering, No. 5/2012. Gdansk University of Technology Publishers, Gdansk 2012.
14. P. Sliwinski: Researches on compensation and valve plate in SM satellite pumps and motors type (in Polish). Hydraulika i Pneumatyka, No. 5/2010.
15. P. Sliwinski: Losses and power balance in hydraulic satellite motor supplied with oil and HFA-E emulsion. Hydraulika a Pneumatika, No 1-2/2009.
16. E.N. Viall, Qin Zhang: Spool Valve Discharge Coefficient Determination. Proceedings of the 48th National Conference on Fluid Power, April 4 - 6, 2000, Chicago, Illinois, USA.
17. D. Wu, R. Burton, G. Schoenau, D. Bitner: Modeling of orifice flow rate at very small openings. International Journal of Fluid Power, v.4, No. 1/2003.
18. D. Wu, R. Burton, G. Schoenau: An empirical discharge coefficient model for orifice flow. International Journal of Fluid Power, v.3, No. 3/2002.
19. T. Zloto, D. Sochacki, P. Stryjewski: Analysis of Oil Leaks in a Variable-Height Gap Between the Cylinder Bloc and the Valve Plate in a Piston Pump by Means of Author-Designed Software and CFD Fluent. TEKA Commission of Motorization and Energetics in Agriculture Vol.14, No. 4/2014.
20. Danfoss product catalog *http://products.danfoss.com/power-solutions/*